

Manuscript Number:

Title: PM10 source apportionment applying PMF and chemical tracer analysis to ship-borne measurements in the Western Mediterranean

Article Type: Research Paper

Keywords: PM10, ship emissions, Mediterranean Basin, source apportionment

Corresponding Author: Ms. Maria Chiara Bove,

Corresponding Author's Institution:

First Author: Maria Chiara Bove

Order of Authors: Maria Chiara Bove; Paolo Brotto; Giulia Calzolari; Federico Cassola; Fabrizia Cavalli; Paola Fermo; Jens Hjorth; Dario Massabò; Silvia Nava; Andrea Piazzalunga; Clara Schembari; Paolo Prati

Abstract: A PM10 sampling campaign was carried out on board the cruise ship Costa Concordia during three weeks in summer 2011. The ship route was Civitavecchia-Savona-Barcelona-Palma de Mallorca-Malta (Valletta)-Palermo-Civitavecchia. The PM10 composition was measured and utilized to identify and characterize the main PM10 sources along the ship route through receptor modelling, making use of the Positive Matrix Factorization (PMF) algorithm. A particular attention was given to the emissions related to heavy fuel oil combustion by ships, which is known to be also an important source of secondary sulphate aerosol. Five aerosol sources were resolved by the PMF analysis. The primary contribution of ship emissions to PM10 turned out to be $(12 \pm 4)\%$, while secondary ammonium sulphate contributed by $(35 \pm 5)\%$. Approximately, 60% of the total sulphate was identified as secondary aerosol while about 20% was attributed to heavy oil combustion in ship engines. The measured concentrations of methane sulphonic acid (MSA) indicated a relevant contribution to the observed sulphate loading by biogenic sulphate, formed by the atmospheric oxidation of dimethyl sulphide (DMS) emitted by marine phytoplankton.



Dipartimento di Fisica
UNIVERSITÀ DEGLI STUDI DI GENOVA



Via Dodecaneso 33
I - 16146 GENOVA

Genova, 09/07/15

Tel: +39 010 3536325
Fax: +39 010 314218
Cod.Fisc. 00754150100
<http://www.fisica.unige.it>

To the **Editor in Chief** of Atmospheric Environment

Dear Editor,

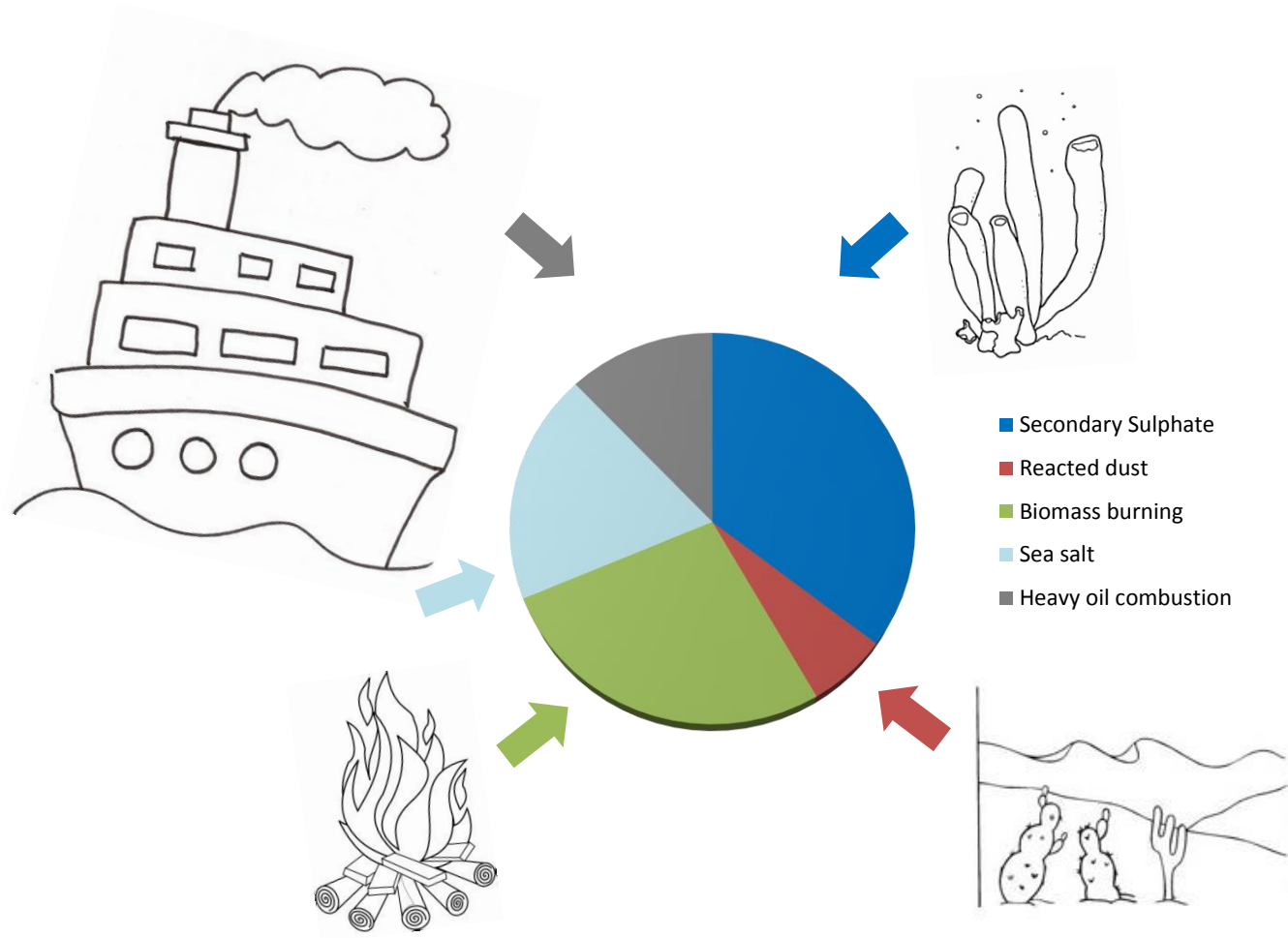
please find in this e-submission the original manuscript:

PM10 source apportionment applying PMF and chemical tracer analysis to ship-borne measurements in the Western Mediterranean

by *Maria Chiara Bove et al.*, submitted for publication in Atmospheric Environment.

With Best Regards

The Corresponding Author
(M.C. Bove)



HIGHLIGHTS

- A conclusive PM₁₀ sampling campaign on a cruise ship was performed in summer 2011
- PMF analysis allowed evaluating the main PM₁₀ sources met along the ship route
- Large marine biogenic sulphur production as function of strong winds
- The new study disentangles primary ship emissions and secondary sulphates
- The contribution of ship emissions was estimated on average: $(12 \pm 4)\%$ of PM₁₀

PM10 source apportionment applying PMF and chemical tracer analysis to ship-borne measurements in the Western Mediterranean

M.C. Bove¹, P. Brotto¹, G. Calzolari³, F. Cassola¹, F. Cavalli², P. Fermo⁴, J. Hjorth², D. Massabò¹, S. Nava³, A. Piazzalunga⁵, C. Schembari², P. Prati¹

¹ Department of Physics, University of Genoa, and INFN, 16146, Genoa, Italy

² Institute for Environment and Sustainability, European Commission, JRC , I-21027, Ispra (VA), Italy

³ Department of Physics and Astronomy, University of Florence, and INFN, 50019, Sesto Fiorentino (FI), Italy

⁴ Department of Chemistry, University of Milan, Milan, 20133, Italy

⁵ Department of Earth and Environmental Sciences, University of Milano Bicocca, 20126, Milan, Italy

Abstract

A PM10 sampling campaign was carried out on board the cruise ship Costa Concordia during three weeks in summer 2011. The ship route was Civitavecchia-Savona-Barcelona-Palma de Mallorca-Malta (Valletta)-Palermo-Civitavecchia. The PM10 composition was measured and utilized to identify and characterize the main PM10 sources along the ship route through receptor modelling, making use of the Positive Matrix Factorization (PMF) algorithm. A particular attention was given to the emissions related to heavy fuel oil combustion by ships, which is known to be also an important source of secondary sulphate aerosol. Five aerosol sources were resolved by the PMF analysis. The primary contribution of ship emissions to PM10 turned out to be $(12 \pm 4)\%$, while secondary ammonium sulphate contributed by $(35 \pm 5)\%$. Approximately, 60% of the total sulphate was identified as secondary aerosol while about 20% was attributed to heavy oil combustion in ship engines. The measured concentrations of methane sulphonic acid (MSA) indicated a relevant contribution to the observed sulphate loading by biogenic sulphate, formed by the atmospheric oxidation of dimethyl sulphide (DMS) emitted by marine phytoplankton.

Keywords: PM10, ship emissions, Mediterranean Basin, source apportionment

1. Introduction

Weather conditions and geographical characteristics make the Mediterranean Basin one of the most polluted regions on Earth in terms of ozone concentrations and aerosol loading (Lelieveld et al, 2002, Velchev et al, 2011). This is caused by local emissions as well as transport of air pollution from outside the Mediterranean region. Ship emissions are an important source of pollution in this region and represent significant and growing contributors to air quality degradation in coastal areas (Van Aardenne et al., 2013). Emissions of exhaust gases and particles from the oceangoing ships affect the chemical composition of the atmosphere, climate and regional air quality (Eyring et al., 2005). In recent years, particle emissions from ships and harbour activities became a concern for air quality and object of several scientific investigations (Moreno et al., 2010, Becagli et al., 2012, Cesari et al., 2014, Bove et al., 2014). A number of studies have shown that ship exhaust particles contain V and Ni and these elements have been used as markers to investigate primary ship emissions using receptor models (Mazzei et al., 2008, Viana et al., 2009; Cuccia et al., 2010, Pandolfi et al., 2011, Salameh et al., 2015). The Joint Research Centre of the European Commission (JRC, EC) has carried out an air quality monitoring program from 2006 to 2014, based on observations from a cruise ship following a regular route in the Western Mediterranean. In the framework of a collaboration agreement between the JRC and Costa Crociere, continuous measurements of atmospheric pollutants were carried out on cruise ships from spring to autumn. During two campaigns in particular, in 2009 and 2010, a two-stage streaker sampler (Formenti et al., 1996) was installed on the ship. The elemental composition of the fine and coarse fraction of PM₁₀, separately collected by the streaker on an hourly basis, was measured by PIXE analysis (Schembari et al., 2014). These datasets were used for an investigation of the influence of ship emissions on the composition of aerosols over the sea through a source apportionment analysis by PMF as well as by chemical marker compounds. The ship emissions were found to be an important source of aerosols in the Western Mediterranean, however a quantification of their impacts by PMF was not obtained. That experiment did not disentangle primary and secondary sources of sulphate and did not resolve the contribution of primary aerosol from ships, presumably because of the insufficient chemical speciation of PM₁₀. A mixed combustion source, which showed evidence of a direct connection with ship emissions was found to contribute by 55%, 63% and 80% to PM₁₀, Black Carbon and sulphate, respectively (Schembari et al., 2014). In summary, the results of

the previous campaigns indicated a significant impact of ship emissions to PM levels in the explored area but were not conclusive. In this context, a new PM₁₀ sampling campaign was organized in the summer of 2011, to complete the information of the previous studies and to get a better description of PM sources. An extensive characterisation of PM₁₀ samples, collected using a sequential filter sampler, was addressed; the obtained data were analysed by PMF and used to identify and characterize the main PM₁₀ sources met along the route.

2. Material and methods

2.1 Monitoring campaign

The monitoring station was placed in a cabin at the front of the top deck of the ship “Costa Concordia”. It permitted to perform continuous measurements of NO_x, SO₂, O₃ and Black Carbon (BC), the last one by means of an Aethalometer (AE 21, 2 wavelengths, Magee Scientific, USA) (Schembari et al., 2014). The aerosol sampling campaigns were carried out during three weeks of summer 2011: July 18-25, August 15-22 and September 12-19. PM₁₀ samples were collected on Quartz filters (47mm diameter, flow rate 2.3 m³ h⁻¹) using a Sven Leckel Ingenieurburo sequential sampler, placed on the top of the cabin where the monitoring and meteorological station were also located. The sampling was carried out on a variable time basis: the sampler was started 1 h after the departure from each harbour and stopped 1 h before the arrival in the next harbour. Each leg was then divided in periods of about 4-5 h with one filter sampled per each period. This resulted in a variable number of filters per open-sea leg and in a total number of about 20 quartz fibre filters per week.

2.2 Analytical methods

All filters were pre-conditioned for two days in a controlled room (temperature: 20±1°C, relative humidity: 50±5%) before and after the sampling and then weighed using an analytical balance (sensitivity: 1 µg). Field blank filters were used to monitor possible artefacts. The compositional analyses were conducted using different methods, depending on the characteristics of the filtering membrane. The elemental composition of filters sampled in August and September weeks, were measured by ED-XRF (Energy Dispersive - X Ray Fluorescence) using an ED-2000 spectrometer from Oxford Instruments (Ariola et al., 2006). For technical reasons, the elemental concentrations in the samples collected during the July cruise were determined instead by PIXE analysis at the HVEE 3 MV Tandetron accelerator, installed at the LABEC (LABoratorio BENi Culturali) laboratory of INFN in Florence

(Calzolari et al., 2006; Lucarelli et al., 2013). The lack of quantification of low-Z elements (Na to P) via ED-XRF (due to the X-ray self-absorption and the high Si concentration in the quartz filters) was partially recovered by Ionic Chromatography analysis. Furthermore, the S and K concentration values determined using ED-XRF were corrected for an average attenuation factor (Bove et al., 2014) to determine their mean values, whereas S, Cl, K resulted to be always below their Minimum Detection Limit when measured by PIXE.

The Organic Carbon (OC) and Elemental Carbon (EC) fractions collected on quartz filters were quantified using the Thermal-Optical Transmittance (TOT) method (Birch and Cary, 1996) with a SUNSET EC/OC instrument while following the EUSAAR_2 protocol (Cavalli et al., 2010).

The filters were finally analysed by Ion Chromatography (IC) using an ICS-1000 Ion Chromatography System (Dionex) at the University of Milan, to determine the water-soluble inorganic components of the particulate matter (Piazzalunga et al., 2013). In particular, for the extraction of the PM, a quarter of each filter was wetted previously and then three times with MilliQ water in an ultrasonic bath for 20 min (complete recovery, $98\% \pm 3\%$), renewing the water at each step. The extracts were analysed using IC to identify the major ionic species (i.e., Na^+ , NH_4^+ , K^+ , Mg^{2+} , Ca^{2+} , Cl^- , SO_4^{2-} , NO_3^-) with an overall 10% uncertainty for the ionic concentrations. The MSA (methane sulfonic acid) concentration values were also measured by IC.

Information on meteorological parameters (wind speed and direction, temperature, humidity from the meteorological station of the ship) and on the ships position, speed and sailing direction, were also available (in 10 min intervals) and used to identify situations where the PM sampling might be influenced by the emissions of Costa Concordia itself. When the inlets of the measurement station were downwind the ship stack within an angle of $\pm 40^\circ$, the data were discarded to avoid any risk of contamination.

Air mass back-trajectories were calculated using the US NOAA HYSPLIT model (<http://ready.arl.noaa.gov/HYSPLIT.php>) with GDAS meteorological data. For each filter, five-day back trajectories arriving at 50 m and 500 m above sea level were calculated for the positions where the filter sampling ended, to evaluate the different air masses arriving over the sea in the three cruise weeks. During summer 2011, the route of the ship was Civitavecchia-Savona-Barcelona-Palma de Mallorca-Malta (Valletta)-Palermo-Civitavecchia (see [Figure E1 in the electronic supplementary material](#)).

2.3 Aerosol composition: mass closure

Details on the method to obtain the aerosol composition is described in Schembari et al. (2014). Briefly, concentration values of SO_4^{2-} , NH_4^+ and NO_3^- were directly retrieved from the IC analysis, while the other aerosol components were obtained from raw data and conversion factors. The sea salt component was calculated from Na and Cl concentration values, taking into account the seawater composition (Seinfeld and Pandis, 1998). The mineral dust component was obtained by multiplication of nssCa^{2+} (nssCa^{2+} , non-sea-salt calcium, i.e. the amount of Ca in excess of the fraction in sea salt) by 5.6, the value retrieved by Putaud et al. (2004) outside of Saharan dust events. Organic Matter (OM) was estimated as $\text{OM} = 1.4 * \text{OC}$, applying the conversion factor from Turpin and Lim (2001). The contributions of different sources to the sulphate concentration was evaluated on the basis of specific markers as described in Schembari et al. (2014). The primary component of the sulphate concentration are the sea salt sulphate, that is the amount of sulphate present in sea salt particles, crustal sulphate, which is the fraction of sulphate in crustal particles (Seinfeld and Pandis, 1998), and primary anthropogenic emissions of sulphate (e.g. from ships). The part of secondary origin, indicated as non-sea-salt sulphate (nssSO_4^{2-}), is defined as the amount of the sulphate present in particles in excess of what expected from sea salt particles, and has two main contributions: anthropogenic and biogenic nssSO_4^{2-} . The biogenic nssSO_4^{2-} was estimated starting from the measurement of MSA concentration in the samples through the relation by Bates et al. (1992), considering the average ambient temperature for each sampling campaign. This estimate has large uncertainties, as discussed by Schembari et al., 2014. The anthropogenic nssSO_4^{2-} was determined as the difference between nssSO_4^{2-} and its biogenic fraction.

2.4 Receptor model-PMF

Positive Matrix Factorization (PMF) was used to identify and characterize the major PM10 sources along the ship route. PMF has been described in detail by its developers (Paatero and Tapper, 1994), it has been adopted in several studies for PM receptor modelling and has rapidly become a reference tool in this research field (e.g., Qin et al., 2006; Escrig et al., 2009; Contini et al., 2012; Cuccia et al., 2013). In this work, the PMF2 program (Paatero, 2010) and the methodology described in Bove et al. (2014) was used. The PMF analyses were carried out using the data collected on Quartz filters from the three weeks of the summer 2011. The variables were selected according to the signal-to-noise criterion (Paatero and Hopke, 2003) and 14 series of concentration values were finally retained for the PMF study: Ti, V, Fe, Ni, MSA, Cl^- , NO_3^- , SO_4^{2-} , Na^+ , NH_4^+ , K^+ , Mg^{2+} , Ca^{2+} , BC. The Polissar et al.

(1998) procedure was used to assign concentration data and their associated uncertainties; the Cl^- , NO_3^- , Na^+ , Mg^{2+} uncertainties only were increased in the PMF runs. The number of samples considered in the PMF run (55) satisfies the criteria set in Thurston and Spengler, 1985. PMF results are affected by the rotational ambiguity (Paatero et al., 2002) and rotations are directly implemented in the minimisation algorithm using the FPEAK parameter (Paatero, 1997). In the analysis, the parameters obtained from the scaled residual matrix, IM (the maximum individual column mean), and IS (the maximum individual column standard deviation), together with Q-values (goodness of fit parameter) were examined to find the most reasonable solution. The best rotation for each factor was chosen in the FPEAK range from -2 to +2 by discarding the solutions corresponding to profiles without physical meaning (i.e., the sum of elemental concentrations exceeded 100%) and selecting those generating concentration ratios between the tracer elements of the natural sources (e.g., sea salt, crustal matter) comparable to literature values (Bove et al., 2014).

3. Results and discussion

3.1 Meteorological conditions

The sea level pressure composite mean and anomalies over the Mediterranean basin during the three campaigns according to the NCEP/NCAR Reanalysis (Kalnay et al. 1996), are shown in [Figure E2 in the electronic supplementary material](#). While in August and in September the synoptic conditions were characterized by the expansion towards the Mediterranean of the Azores Anticyclone, in line with seasonal climatology (especially in August, whereas a slightly negative anomaly is found in September), in July the situation was very peculiar. In this case, the anticyclonic system is confined over the Atlantic, favouring the development of low-pressure systems across Central Europe and the Mediterranean Basin, where a strong negative pressure anomaly can be seen.

The meteorological parameters recorded during the three cruises by the on-board instrumentation are reported in Figure 1 and confirm what is suggested by the synoptic analysis. In particular, pressure exhibited lower average values and larger variability in July, associated to episodes of strong wind and, as a consequence, rough sea along the route. On the contrary, during the two campaigns in August and September, more stable conditions were encountered, with higher pressure values and generally lighter winds, apart from the last leg of the September cruise, when the passage of an Atlantic frontal system determined a sudden pressure drop and wind speed increase.

The meteorological conditions along the ship route during the most relevant strong wind episodes were also assessed using a 32-year hindcast, recently realized at the University of Genoa by means of simulations with the Weather Research and Forecasting (WRF, Skamarock et al. 2008) model on a domain covering the entire Mediterranean with a horizontal grid spacing of 10 km. Details about the modelling system are given in Mentaschi et al. (2015).

3.2 PM10 composition

The average PM10 concentration and its composition are reported in Table 1. The analysed species amount, on average, to 91% ($\pm 5\%$ relative standard deviation) of PM10. The secondary compounds, which account, on average, for approximately 40% of PM10, are the most abundant species. Sulphate is well correlated with ammonium concentrations ($r^2=0.9$), however the ionic balance shows some differences between the three campaigns. A detailed analysis of ionic fraction reveals that PM10 in July was characterized by a clear presence of sulphate not balanced by ammonium (Figure 2), in coincidence with a lower $\text{SO}_4^{2-}/\text{Mg}^{2+}$ molar ratio. The PM10 chemical composition is shown in Figure 3, separately for the three 2011 cruises. Actually, the nssSO_4^{2-} , NO_3^- , sea salt and organic components seem to be quite different between the July campaign and the other two cruise weeks. Such a discrepancy is attributable to the peculiar meteorological conditions occurred in July, as discussed in the previous section. The back trajectory analysis indicated that the air masses reaching the ship route in July, had been mainly over the sea for at least the previous 24 h. During the August and September cruises, the impacting air masses passed mostly over the continental areas, suggesting a larger contribution from the transport of terrestrial pollutants to the open sea. An example is shown in [Figure E3 of the electronic supplementary material](#).

Organic aerosol represents only a minor fraction of PM10: some technical problems in the thermo-optical analysis, in particular with the samples of the July cruise, made anyway OC values not sufficiently firm. However, it is worth noting that the sampling of organic aerosol can be subject to positive and negative artefacts (Turpin et al., 2000; Vecchi et al., 2009). Indeed, some samples are present, in which large differences are found between the PM10 mass and the sum of the chemical components (Figure 3); this could be partly explained by the above noted difficulties of measuring OC.

EC values showed generally a very good correlation with BC concentration monitored by the Aethalometer but in July, probably due to lower concentration values ([see Figure E4 in](#)

[the electronic supplementary material](#)). BC values measured by the Aethalometer were only retained and utilised in the PMF database for the whole period.

The primary contribution of ship emissions to PM10 can be calculated on the basis of previous research works (Agrawal et al., 2009; Pandolfi et al., 2011, Zaho et al., 2013) and using the equation:

$$PM_a = R \frac{V_a}{F_{V,HFO}} \quad (1)$$

The value of the constant $R = 8205.8$, suggested in Agrawal et al. (2009), is internationally adopted in locations with HFO-burning ship emissions. V_a is the ambient concentration of V (ng m^{-3}), whilst $F_{V,HFO}$ is a term indicating the typical V content (in ppm) in HFOs used by vessels. We used the typical value of $F_{V,HFO} = (65 \pm 25)$ ppm, so far used to calculate the contribution of ship emissions in the harbour site of Brindisi (Cesari et al., 2014). According to eq. (1), the primary PM10 from ship traffic ranged from 0.7 to $3.4 \mu\text{g m}^{-3}$; similar values had been previously obtained in some port sites (Viana et al., 2009).

3.3 Sulphate apportionment

The sources of sulphate can be apportioned in terms of specific categories as described in Section 2.3: ssSO_4^{2-} and nssSO_4^{2-} . The latter can be further divided in crustal ($\text{nssSO}_4^{2-}_{\text{crust}}$), biogenic ($\text{nssSO}_4^{2-}_{\text{bio}}$) and anthropogenic ($\text{nssSO}_4^{2-}_{\text{antr}}$). With this approach, total SO_4^{2-} is apportioned using marker compounds as described in Schembari et al. (2014). Average results of the 2011 campaign are reported in Table 2. Large concentration values of nssSO_4^{2-} were obtained for all the three weeks, while highest values of ssSO_4^{2-} and lowest values of nssSO_4^{2-} were observed in July (Figure 3). The latter were in coincidence with a quite high wind speed, in particular during the Savona-Barcelona and Palermo-Civitavecchia legs. The analysis of wind speed and direction, both measured on board and obtained by hindcast simulations with the WRF-ARW model (see also [Figure E5 and E6 in the electronic supplementary material](#)), highlighted that it blew from the sea and its velocity increased rapidly during the last part of the routes, close to the Barcelona coast and to Civitavecchia, respectively. This observation confirms the sea salt dependence on the local wind speed as discussed in many studies, for the Mediterranean Basin in particular by Bergametti et al. (1989a) and Chabas and Lefèvre (2000). The main contribution to nssSO_4^{2-} was of anthropic origin in August and September, whereas in July $\text{nssSO}_4^{2-}_{\text{bio}}$ was prevailing, probably due to the particular meteorological

conditions that determined high sea salt concentrations. The nssSO_4^{2-} _{anthr} contributed to PM10 by 9%, 15% and 22%, in July, August and September, respectively, while the nssSO_4^{2-} _{bio} was on average 11%, 14% and 4% of PM10 in the same periods. The nssSO_4^{2-} _{crust}, as estimated by this approach, remained always around 1% of PM10.

During the three cruises, no clear correlations between the MSA concentration values and MSA/ nssSO_4^{2-} concentration ratios were observed (maximum correlation in July, $R^2 = 0.4$, see Figure 4). The low MSA/ nssSO_4^{2-} ratios observed in August and September could be attributed to the influence of air masses containing anthropogenic sulphate from the nearby continents (Section 3.2), as described by Chen et al. (2012). The lowest MSA/ nssSO_4^{2-} ratio (ratio = 0.005) was found in August along the Malta-Palermo leg, together with the highest nssSO_4^{2-} concentration value. The back-trajectory analysis indicates that in this leg the ship was impacted by air masses that previously passed over Tripoli, the most populous city of Libya; however this leg is also a naval route at high traffic level in the Mediterranean Basin (Figure 5). On the contrary, the highest MSA/ nssSO_4^{2-} molar ratio of 0.11, observed in July, was associated with the air sample with highest MSA concentration value and air masses coming from the sea as indicated by back-trajectory analyses (Figure 5).

The above-discussed results can be compared with those collected in the similar cruises in 2009-2010 (Schembari et al., 2014). The previous sulphate apportionment showed similar contributions to 2011 data for nssSO_4^{2-} _{crust} and ssSO_4^{2-} . Most of the sulphate was assigned to anthropogenic influences while the biogenic contribution was found to be important, but influenced by large uncertainties. The nssSO_4^{2-} _{anthr} showed comparable contributions to values obtained in 2011, while lower values of nssSO_4^{2-} _{bio} were obtained in the 2009-2010 chemical analysis.

3.4 PMF results

The database used as input to PMF included data obtained by the analysis of filters sampled along open-sea legs while samples collected when the ship was manoeuvring or hotelling in the harbours and when the sampling station was downwind the ship stack, were excluded. The database was completed with the time series of hourly BC concentration values and PM10 mass concentration.

Five factors were resolved and identified by PMF for PM10: *Secondary Sulphate*, *Reacted dust*, *Biomass burning*, *Sea salt* and *Heavy oil combustion*. Source profiles and explained variations (EV) parameters are shown in Figure 6, while the average PM10 apportionment is given in Figure 7.

PMF-Factor 1 was identified as the contribution due to *Secondary Sulphate* looking at the high EVs for SO_4^{2-} and NH_4^+ and the relevance of these compounds in the chemical profile (Figure 6). The average concentration ratio for $\text{SO}_4^{2-}:\text{NH}_4^+$ in the factor is 2.1 ± 0.1 , which is slightly lower than the stoichiometric figure for ammonium sulphate (i.e. $\text{SO}_4^{2-}:\text{NH}_4^+ = 2.7$). A very similar profile for *Secondary Sulphate* had been already observed at a Central Mediterranean site, namely in the town of Lecce (IT), by Perrone et al. (2013). The source profile is also comparable with another profile obtained by a study performed along a route across the Mediterranean from Barcelona to Istanbul during March and April, 2008 (Moreno et al., 2010). The average relative contribution of this factor to the PM10 mass is $(35 \pm 5)\%$, with highest concentrations observed during August and lowest in July as reported in Table 3. The PMF result is comparable, within its uncertainty, with the direct calculation of the average abundance of ammonium non-sea-salt sulphate in PM10 of $(39 \pm 4)\%$, discussed in Section 3.2. The quite low concentration value of July confirms the observation of sea salt events that reduce the relative importance of the contribution by secondary aerosols, as reported in Section 3.2.

PMF-Factor 2 was characterised by high EV values for Ti and Fe, this suggesting a contribution by mineral dust, and by a relevant fraction of SO_4^{2-} , NO_3^- , NH_4^+ and BC in the source profile (Figure 6). The mineral particles aged in the atmosphere and then changed their original composition, getting mixed/coated with organic and inorganic ions (sulphate and nitrate) and BC (Fairlie et al., 2010). For this reason, this factor was labelled as *Reacted dust*, also in agreement with other source profiles obtained by PMF in Mediterranean sites (Perrone et al., 2013, Cesari et al., 2014). The temporal pattern of this factor showed highest concentrations along the Barcelona-Palma legs (see also [Figure E7 in the electronic supplementary material](#)), in particular near the Palma coast. Moreover, this source profile is quite similar to the mineral dust profile obtained by PMF analysis of the data sampled in a site located at Palma de Mallorca (Pey et al., 2013), which includes anthropogenic dust emissions from the harbour too. The fraction of PM10 attributed by PMF to *Reacted dust* was $(6 \pm 1)\%$, in pretty good agreement with the “chemical” apportionment of $(10 \pm 3)\%$ reported in Section 3.2.

PMF-Factor 3 was assigned to *Biomass burning* because it was characterized by high contributions of BC, SO_4^{2-} , NH_4^+ and K^+ in the source profile (Figure 6) and by high EV values for BC and K^+ . This choice is in agreement with other works which adopted K^+ as tracer of biomass burning (Belis et al., 2011). High concentration values were detected along the Malta-Palermo leg, both in August and September (see also [Figure E7 in the electronic](#)

[supplementary material](#)). Maximum values were observed with high wind speed and prevailing direction from the Sicilian coast and from the city of Palermo. This source contributed on average to $(27 \pm 5)\%$ of PM₁₀, ranging from 10% to 33% during the three cruises (Table 3).

PMF-Factor 4 was identified as *Sea salt* since it was characterized by high EV values for NO_3^- , Cl^- , Na^+ , Mg^{2+} and MSA (Figure 6). The $\text{Cl}^-:\text{Na}^+$ ratio in the profile is equal to 0.2, which is much smaller than the 0.9 mean ratio obtained in the 2009 and 2010 cruises (Schembari et al., 2014) and than the 1.8 ratio of fresh sea salt particles (Seinfeld and Pandis, 1998). This can be due to evaporation of HCl to the atmosphere which occurs at Mediterranean sites (Perrone et al., 2013, Cuccia et al., 2013). The PMF algorithm could not distinguish fresh and aged sea salt: in the *Sea salt* source profile (Figure 6), the presence of the secondary nitrates and MSA^- due to the oxidation of dimethyl sulphide emitted from the sea suggested the mixing with a secondary marine source. The average fraction of PM₁₀ attributed to this factor was $(19 \pm 4)\%$, in agreement with the $(27 \pm 5)\%$ value obtained as the sum of Sea salt and Nitrates components obtained evaluated by chemical analysis (Section 3.2). The sea salt concentration was higher in July than in August and September as highlighted in Table 3: this confirms the occurrence of sea salt events during the Savona-Barcelona and Palermo-Civitavecchia legs as described in Section 3.2.

PMF-Factor 5 was finally identified as *Heavy oil combustion* because it was characterized by high EV values for V and Ni, typical tracers of heavy oil combustion (Mazzei et al., 2008, Viana et al., 2009). The V:Ni concentration ratio in the source profile is 2.6 ± 0.1 , in agreement with the 2.9 ± 0.4 value obtained by PMF during the previous campaigns (Schembari et al., 2014) and with the conclusions of several other literature works which recognized such value as typical of ship emissions (Agrawal et al., 2008, Mazzei et al., 2008, Cuccia et al., 2010, Pandolfi et al., 2011, Bove et al., 2014). The source profile was enriched in sulphate with $\text{SO}_4^{2-}:\text{V} = 67 \pm 4$. The initial $\text{SO}_4^{2-}:\text{V}$ ratio in the particulate exhaust (PM_{2.5}) of the main engine of different oceangoing container vessels is reported to be in the range 11–27 (Agrawal et al., 2008). However, the amount of SO_4^{2-} in the air mass is expected to grow fast due to SO_2 conversion into sulphate; this conversion is faster in high UV radiation and high humidity conditions (Restad et al., 1998, Becagli et al., 2012). Actually, the measured $\text{SO}_4^{2-}/\text{V}$ ratio (similar to the $\text{SO}_4^{2-}:\text{V}$ ratio in the profile) is lower in July than the other two cruise weeks, confirming the higher marine contribution and therefore of the ship emissions in this period. Ship emissions contributed on average to $(12 \pm 4)\%$ of PM₁₀. This

figure is in agreement with the $(16 \pm 11)\%$ percentage evaluated considering the measured V as a marker for the combustion in ship engines (3.2 Section).

The apportionment of single PM10 species is given in Figure 8. Notably, NO_3^- was mainly associated with *Sea salt* (on average 95%) supporting the nature of secondary marine source, whereas NH_4^+ was primarily associated with one of the secondary components of PM10, i.e. *Secondary Sulphate* (on average: 80%). On average, $(23 \pm 9)\%$ of the SO_4^{2-} was attributed to *Heavy oil combustion*. The Sulphate apportionment resolved by PMF appears to be different in the three cruises (see also [Figure E8 in the Electronic supplementary material](#)). The apportionment seems to be quite similar in August and September while an increase of the total SO_4^{2-} attributed to *Heavy oil combustion* in association with the Sea salt events (3.2 Section) was observed in July. The latter can be explained by the possible contamination in the *Heavy oil combustion* profile of the biogenic fraction of the sulphates (the measured biogenic sulphate was much larger than the anthropogenic one in July); this is compatible with the expectation that both sources are predominantly marine. Moreover, the average measured $\text{MSA}/\text{nssSO}_4^{2-}$ ratio of 0.03 for the three cruise weeks is the same value found in the *Heavy oil combustion* factor obtained by PMF analysis to support the biogenic contamination of the sulphate in the profile.

3.3.1 Sources comparison

The new study has provided more complete and clear information than the analysis performed in the past years (Schembari et al., 2014). Due to the lack of a complete chemical speciation, only four sources were resolved in 2010 and in particular the PMF did not resolve secondary and primary sources of sulphate. A *Combustion* source only, which showed evidence of a contribution by ship emissions, was found to contribute by $(55 \pm 4)\%$ to PM10. The main scope of the 2011 experiment was to separately quantify the contribution of ship emissions and of secondary sulphate to PM10. This objective was achieved: in 2011 the *Secondary Sulphate* and *Heavy oil combustion* were found to account for $(35 \pm 5)\%$ and $(12 \pm 4)\%$ of PM10, respectively. The *Combustion* factor identified in the previous campaigns is comparable with the sum of *Secondary Sulphate* and *Heavy oil combustion* sources in 2011. Moreover, the source *Not identified* by PMF in 2009-2010 has been recognized as *Biomass burning* with the 2011 dataset because it is characterized by the same tracer elements and high contributions of BC and K^+ . The *Sea salt* source shows similar mean values of the PM10 apportionment even if higher contribution values were observed in the July week in 2011, for meteorological reasons (intense winds) and probably also because the old PMF data set did

not include nitrates, which are a significant component of the aged sea salt. The *Reacted dust* factor shows the same source profile and mean contribution to PM10 as obtained in 2010.

The names given to the sources of the five PMF factors obviously represent a simplification; it is clear that there must be several additional minor sources that have contributed to the observed aerosol composition; in particular, land-based traffic and industrial sources. For this reason, the relative contribution attributed to ship emissions must be seen as an upper limit. On the other hand, due to the high Sulphur content of the HFO used by ships and correspondingly high SO₂ emissions, ship emissions will also contribute to the PMF category *Secondary Sulphate*.

4. Conclusions

PM10 aerosol samples collected during three campaigns on board a cruise ship from July to September 2011 were analysed to determine their chemical composition and to improve the source apportionment obtained during previous studies performed on board cruise ships in the Western Mediterranean. The biogenic fraction of the sulphate was prevailing during the July campaign, together with a higher contribution of the ship emissions, probably due to the particular meteorological conditions along the ship route with the most relevant strong wind episodes that determined high sea salt concentrations. Five sources were resolved and identified by PMF analysis with the new data sets: *Secondary Sulphate*, *Reacted dust*, *Biomass burning*, *Sea salt* and *Heavy oil combustion*. Heavy oil combustion by ship engines was identified using V and Ni as tracers. Secondary ammonium sulphate was found to be an important source of aerosol in Western Mediterranean. The experiment allowed the identification of a contribution of primary ship emissions to PM10. This contribution turned out to be $(12 \pm 4)\%$, while secondary ammonium sulphate contributed by $(35 \pm 5)\%$. Approximately 60% of the total sulphate was attributed to secondary sources and around 20% was attributed to *Heavy oil combustion* considering the measuring campaigns not influenced by strong sea salt events.

Acknowledgements

Thanks are due to Costa Crociere and to the technical assistance of V. Ariola from the Department of Physics of the University of Genoa. This work has been partially supported by INFN under the grant for the MANIA experiment.

References

Agrawal, H., Welch, W.A., Miller, J.W., Cocker, D.R., 2008. Emission measurements from a crude oil tanker at sea. *Environmental Science Technology* 42, 7098-7103.

Agrawal, H., Eden, R., Zhang, X., Fine, P.M., Katzenstein, A., Miller, J.W., et al. 2009. Primary particulate matter from ocean-going engine in the southern California air basin. *Environmental Science Technology* 43, 398–402.

Ariola, V., D'Alessandro, A., Lucarelli, F., Marcazzan, G., Mazzei, F., Nava, S., Garcia Orellana, I., Prati, P., Valli, G., Vecchi, R., Zucchiatti, A. 2006. Elemental characterization of PM₁₀, PM_{2.5} and PM₁ in the town of Genoa (Italy). *Chemosphere* 62, 226-232.

Bates, T., Calhoun, J., Wang, Y., Quinn, P., 1992. Variations in the methanesulphonate to sulphate molar ratio in submicrometer marine aerosol particles over the south pacific ocean. *Journal of Geophysical research* 97, 9859-9865.

Becagli, S., Sferlazzo, D.M., Pace, G., Di Sarra, A., Bommarito, C., Calzolari, G., et al. 2012. Evidence for heavy fuel oil combustion aerosols from chemical analyses at the island of Lampedusa: a possible large role of ships emissions in the Mediterranean. *Atmospheric Chemistry and Physics* 12, 3479–92.

Belis, C.A., Cancelinha, J., Duane, M., Forcina V, Pedroni V, Passarella R, et al. Sources for PM air pollution in the Po Plain, Italy, 2011 I. Critical comparison of methods for estimating biomass burning contributions to benzo(a)pyrene. *Atmospheric Environment* 45, 7266–75.

Belis C.A., Karagulian, F., Larsen, B.R., Hopke, P.K, 2013. Critical review and meta-analysis of ambient particulate matter source apportionment using receptor models in Europe. *Atmospheric Environment* 69, 94-108.

Bergametti, G., Dutot, A.-L., Buat-Menard, P., Losno, R., and Remoudaki, E., 1989a. Seasonal variability of the elemental composition of atmospheric aerosol particles over the north western Mediterranean, *Tellus* 41B, 353–361.

Birch, M. E., Cary, R. A., 1996. Elemental carbon-based method for monitoring occupational exposures to particulate diesel exhaust. *Aerosol Science and Technology* 25, 221-241.

Bove, M.C., Brotto, P., Cassola, F., Cuccia, E., Massabò, D., Mazzino, A., Piazzalunga, A., Prati, P., 2014. An integrated PM_{2.5} source apportionment study: Positive Matrix Factorisation vs. the Chemical Transport Model CAMx. *Atmospheric Environment* 94, 274-286.

Calzolari, G., Chiari, M., García Orellana, I., Lucarelli, F., Migliori, A., Nava, S., Taccetti, F., 2006. The new external beam facility for environmental studies at the Tandatron accelerator of LABEC. *Nuclear Instrument Methods B249 (1-2)*, 928-931.

Cavalli, F., Putaud, J.P., Viana, M., Yttri, K.E., Gemberg, J., 2010. Toward a standardised thermal-optical protocol for measuring atmospheric organic and elemental carbon: the EUSAAR protocol. *Atmospheric Measurement Techniques* 3, 79-89.

Cesari, D., Genga, A., Ielpo, P., Siciliano, M., Mascolo, G., Grasso, F.M., Contini, D., 2014. Source apportionment of PM_{2.5} in the harbour-industrial area of Brindisi (Italy): Identification and estimation of the contribution of in-port ship emissions. *Science of the Total Environment* 497-498, 392-400.

Chabas, A. and Lefèvre, R. A., 2000. Chemistry and microscopy of atmospheric particulates at Delos (Cyclades-Greece). *Atmospheric Environment* 34, 225-238.

Chen, L. Wang, J., Gao, Y., Xu, G., Yang, X., Lin, Q., Zhang, Y., 2012. Latitudinal distributions of atmospheric MSA and MSA/nss-SO₄²⁻ ratios in summer over the high latitude regions of the Southern and Northern Hemispheres. *Journal of geophysical research* 117, D10306, doi:10.1029/2011JD016559.

Chiari, M., Lucarelli, F., Mazzei, F., Nava, S., Paperetti, L., Prati, P., Valli, G., Vecchi, R. 2005. Characterization of airborne particulate matter in an industrial district near Florence by PIXE and PESA. *X-Ray Spectrometry* 34, 323-329.

Chow, J.C., Watson, J.G., 1999. Ion chromatography in elemental analysis of airborne particles. In: Landsberger, S., Creatchman, M. (Eds.), *Elemental Analysis of Airborne Particles*, vol. 1. Gordon and Breach Science, Amsterdam, 97-137.

Contini, D., Belosi, F., Gambaro, A., Cesari, D., Stortini, A., Bove, M.C., 2012. Comparison of PM10 concentrations and metal content in three different sites of the Venice Lagoon: an analysis of possible aerosol sources. *Journal of Environmental Science* 24 (11), 1954-1965.

Cuccia, E., Bernardoni, V., Massabò, D., Prati, P., Valli, G., Vecchi, R., 2010. An alternative way to determine the size distribution of airborne particulate matter. *Atmospheric Environment* 44, 3304-3313.

Cuccia, E., Massabò, D., Ariola, Bove, M.C., Fermo, P., Piazzalunga, A., Prati, P., 2013. Size resolved comprehensive characterization of airborne particulate matter. *Atmospheric Environment* 67, 14-26.

Eyring, V., Köhler, H.W., Van Aardenne, J., Lauer, A., 2005. Emissions from international shipping: 1. The last 50 years. *Journal of Geophysical Research Atmosphere* 110, D17305.

Escrig, A., Monfort, E., Celades, I., Querol, X., Amato, F., Mingiullon, M.C., Hopke, P.K., 2009. Application of optimally scaled target factor analysis for assessing source contribution of ambient PM10. *Journal of Air Waste Management Association* 59, 1296-1307.

Fairlie, T.D., et al., 2010. Impact of mineral dust on nitrate, sulphate, and ozone in transpacific Asian pollution plumes. *Atmospheric Chemistry and Physics* 10, 3999-4012.

Formenti, P., Prati, P., Zucchiatti, A., Lucarelli, F., Mandò, P.A., 1996. Aerosol study in the Genova area via a two stage streaker and PIXE analysis. *Nuclear Instrument Methods B113*, 359-362.

Kalnay, E., Kanamitsu, M., Kistler, R., Collins, W., Deaven, D., Gandin, L., Iredell, M., Saha, S., White, G., Woollen, J., Zhu, Y., Leetmaa, A., Reynolds, R., Chelliah, M., Ebisuzaki, W., Higgins, W., Janowiak, J., Mo, K. C., Ropelewski, C., Wang, J., Jenne, R., Joseph, D., 1996.

The NCEP/NCAR 40-Year Reanalysis Project, *Bulletin of the American Meteorological Society* 77, 437-471.

Lelieveld, J., Berresheim, H., Borrmann, S., Crutzen, P.J., Dentener, F., 2002. Global air pollution crossroads over the Mediterranean. *Science* 298, 794-799.

Lucarelli, F., Calzolari, G., Chiari, M., Giannoni, M., Mochi, D., Nava, S., Carraresi, L., 2013. The upgraded external-beam PIXE/PIGE set-up at LABEC for very fast measurements on aerosol samples. *Nuclear Instruments and Methods in Physics Research*. <http://dx.doi.org/10.1016/j.nimb.2013.05.099>.

Mazzei, F., D'Alessandro, A., Lucarelli, F., Nava, S., Prati, P., Valli, G., Vecchi, R., 2008. Characterization of particulate matter sources in an urban environment. *Science of Total Environment* 401, 81-89.

Mentaschi, L., Besio, G., Cassola, F., Mazzino, A., 2015. Performance evaluation of WavewatchIII in the Mediterranean Sea. *Ocean Modelling* 90, 82-94.

Moreno, T., Perez, N., Querol, X., Amato, F., Alastuey, A., Bhatia, R., Spiro, B., Hanvey, M., Gibbons, W., 2010. Physicochemical variations in atmospheric aerosols recorded at sea on board the Atlantic-Mediterranean 2008 Scholar Ship cruise (Part II): natural versus anthropogenic influences revealed by PM10 trace element geochemistry. *Atmospheric Environment* 44, 2563-2576.

Pandolfi, M., Gonzalez-Castanedo, Y., Alastuey, A., De la Rosa, J., Mantilla, E., Sanchez de la Campa, A., et al. 2011. Source apportionment of PM10 and PM2.5 at multiple sites in the strait of Gibraltar by PMF: impact of shipping emissions. *Environment Science Pollution Research* 28, 260-9.

Paatero, P., Tapper, U., 1994. Positive matrix factorization: a non-negative factor model with optimal utilization of error estimates of data values. *Environmetrics* 5, 111-126.

Paatero, P., 1997. Least squares formulation of robust, non-negative factor analysis. *Chemometrics Intelligent Laboratory Systems* 37, 23-35.

Paatero, P., Hopke, P.K., Song, X.H., Ramadan, Z., 2002. Understanding and controlling rotations in factor analytic models. *Chemometrics and Intelligent Laboratory Systems* 60, 253-264.

Paatero, P., Hopke, P.K., 2003. Discarding or down weighting high-noise variables in factor analytic models. *Analytica Chimica Acta* 490, 277-289.

Paatero, P., 2010. User's Guide for Positive Matrix Factorization Programs PMF2 and PMF3, Part 1: Tutorial. University of Helsinki, Finland.

Perrone, M.R., Becagli, S., Garcia Orza, J.A., Vecchi, R., D'Inno, A., Udisti, R., Cabello, M., 2013. The impact of long-range-transport on PM1 and PM2.5 at a Central Mediterranean site. *Atmospheric Environment* 71, 176-186.

Pey, J., Alastuey, A., Querol, X., 2013. PM10 and PM2.5 sources at an insular location in the western Mediterranean by using source apportionment techniques. *Science of the total Environment* 456-457, 267-277.

Piazzalunga, A., Bernardoni, V., Fermo, P., Vecchi, R., 2013. Optimisation of analytical procedures for the quantification of ionic and carbonaceous fractions in the atmospheric aerosol and applications to ambient samples. *Analytical and Bioanalytical Chemistry* 405, 1123-1132.

Putaud, J.P., Van Dingenen, R., Dell'Acqua, A., Raes, F., Matta, E., Decesari, S., Facchini, M.C., Fuzzi, S., 2004. Size-segregated aerosol mass closure and chemical composition in Monte Cimone (I) during MINATROC. *Atmospheric Chemistry and Physics* 4, 889-902.

Polissar, A.V., Hopke, P.K., Paatero, P., Malm, W.C., Sisler, J.F., 1998. Atmospheric aerosol nucleation and primary emission rates. *Atmospheric Chemistry and Physics*, 1339-1356.

Qin, Y., Kim, E., Hopke, P.K., 2006. The concentration and sources of PM2.5 in metropolitan New York City. *Atmospheric Environment* 40, 312-332.

Restad, K., Isaksen, I. S. A., and Berntsen, T. K., 1998. Global distribution of sulphate in the troposphere: A three-dimensional model study. *Atmospheric Environment* 32, 3593–3609.

Salameh, D., Detournay A., Pey, J., Pérez, N., Liguori, F., Saraga D., Bove, M.C., Brotto P, Cassola F., Massabò, D., Latella A., Pillon, S., Formenton, G., Patti, S., Armengaud, A., Piga, D. Jaffrezoj, J.L. Bartzisf, J., Tolis, E., Prati, P. Querol, X., Worthama, H., Marchand, N., 2015. PM2.5 chemical composition in five European Mediterranean cities: A 1-year study. *Atmospheric research* 155, 102-117.

Schembari, C., Bove, M.C., Cuccia, E., Cavalli, F., Hjorth, J., Massabò, D., Nava, S., Udisti, R., Prati, P. 2014. Source apportionment of PM10 in the Western Mediterranean based on observations from a cruise ship. *Atmospheric Environment* 98, 510-518.

Seinfeld, J.H., Pandis, S.N., 1998. *Atmospheric Chemistry and Physics*. John Wiley and Sons.

Skamarock, W.C., Klemp, J.B., Dudhia, J., Gill, D.O., Barker, D.M., Huang, X.Z., Wang, W., Powers, J.G., 2008. A Description of the Advanced Research WRF Version 3. Technical report. Mesoscale and Microscale Meteorology Division, NCAR, Boulder, Colorado.

Thurston, G.D., Spengler, J.D., 1985. A quantitative assessment of source contributions to inhalable particulate matter pollution in metropolitan Boston. *Atmospheric Environment* 19, 9-25.

Turpin, B.J., Saxena, P., Andrews, E., 2000. Measuring and simulating particulate organics in the atmosphere: problems and prospects. *Atmospheric Environment* 34, 2983-3013.

Turpin, B.J., Lim, H.J., 2001. Species contributions to PM2.5 mass concentrations: Revisiting common assumptions for estimating organic mass. *Aerosol Science Technology* 35 (1), 602-610.

Van Aardenne, J., A. Colette, B. Degraeuwe, P. Hammingh, M. Viana, I. de Vlieger, 2013. The impact of international shipping on European air quality and climate forcing. EEA Technical Report no. 4.

Vecchi, R., Valli, G., Fermo, P., D'alessandro, A., Piazzalunga, A., Bernardoni, V., 2009. Organic and inorganic sampling artefacts assessment. *Atmospheric Environment* 43, 1713-1720.

Velchev, K., Cavalli, F., Hjorth, J., Vignati, E., Dentener, F., Raes, F., 2011. Ozone over Western Mediterranean Sea-results from two years of shipborne measurements. *Atmospheric Chemistry and Physics* 11, 675-688.

Viana, M., Amato, F., Alastuey, A., Querol, X., 2009. Chemical Tracers of particulate emissions from commercial shipping. *Environmental Science Technology* 43, 7472-7477.

Zhao, M., Zhang, Y., Maa, W., Fu, Q., Yang, X., Li, C., et al. 2013. Characteristics and ship traffic source identification of air pollutants in China's largest port. *Atmospheric Environment* 64, 277-86.

FIGURE AND TABLE CAPTIONS

Figure 1. Times series of temperature, relative humidity and pressure (top), and wind speed (bottom) recorded by the meteorological instrumentation on board the ship during the three campaigns.

Figure 2. Ionic balance for the three cruise campaigns (top) together with $\text{SO}_4^{2-}/\text{Mg}^{2+}$ molar ratio (bottom).

Figure 3. PM10 chemical composition obtained from raw data and conversion factors during July (top), August (centre) and September (bottom) campaigns.

Figure 4. Correlations between MSA and $\text{MSA}/\text{nssSO}_4^{2-}$ observed during the July cruise campaign in summer 2011.

Figure 5. Air mass back trajectories (AMBTs) calculated from the National Oceanic and Atmospheric Administration (NOAA) GDAS meteorology database, using the Hybrid Single-Particle Lagrangian Integrated Trajectories (HYSPLIT) model. Five-day AMBTs were obtained at 50 and 500 m height levels over the sampling locations every six hours: (top) related to the lowest $\text{MSA}/\text{nssSO}_4^{2-}$ ratio observed on 19 August during the August cruise

week; (bottom) related to the highest $\text{MSA}/\text{nssSO}_4^{2-}$ ratio observed on 19 July during the July cruise week.

Figure 6. PMF profiles (left axis, grey bars) and explained variation factors, EV (right axis, white circles) of the PM10 sources resolved in all the three cruise weeks in summer 2011.

Figure 7. Average source apportionment obtained by the PMF analysis of the PM10 data sets collected during the summer 2011.

Figure 8. Average apportionment of elements/compounds concentration obtained by PMF analysis calculated with the PM10 data sets of the whole field campaign.

Table 1. Average PM10 composition and BC obtained by Aethalometer for the three campaigns in summer 2011: average (A) and standard deviation (St. Dev) of concentration values were calculated with the samples (reported as percentage frequency, F) with concentration values above their Minimum Detection Limit (MDL). For K and Ca both the total concentration by ED-XRF and the soluble fraction by IC are reported.

Table 2. Contributions (sea salt sulphate, ssSO_4^{2-} ; non-sea-salt sulphate, nssSO_4^{2-} : crustal, biogenic, anthropogenic) to the total SO_4^{2-} concentration, determined from chemical marker compounds, for the three cruise weeks.

Table 3. Average source apportionment obtained by the PMF analysis of the PM10 data sets collected during the summer 2011 separately for the three cruise campaigns. The average source apportionment is reported in absolute and relative values.

Electronic supplement material

Figure E1. Route of Costa Concordia during the three campaigns in summer 2011.

Figure E2. Sea level pressure composite mean (left) and anomalies (right) with respect to the 1981-2010 climatology for the July (top panel), August (center) and September (bottom) campaigns, obtained from the NCEP/NCAR Reanalysis (images provided by the NOAA/ESRL Physical Sciences Division, Boulder Colorado, from their web site at <http://www.esrl.noaa.gov/psd/>).

Figure E3. Air mass back trajectories calculated using the HYSPLIT model, related to 21 July (top panel) and 20 August 2011 (bottom).

Figure E4. Correlation between BC measured by Aethalometer and EC by Sunset Analyser in July, August and September cruise weeks.

Figure E5. Time trends of sea salt component of PM10 obtained as described in Section 2 and correlation between wind velocity (km/h) (top figure) and wind prevalent direction (bottom) along the open sea tracks considered.

Figure E6. 10-m wind fields simulated by the non-hydrostatic mesoscale model WRF-ARW relative to the sea salt events: Savona-Barcelona tracks of the July 18 (top) and Palermo-Civitavecchia tracks of the July 24 (bottom).

Figure E7. Time trends of the five pollutant sources (factors) obtained by PMF analysis during the three cruise weeks in summer 2011.

Figure E8. Average apportionment of the total Sulphate compound obtained by PMF analysis calculated with the PM10 data sets for the three cruise 2011 weeks.

Table1

[Click here to download Table: Table1.docx](#)

| ng m ⁻³ | | | |
|-------------------------------|-------|---------|------|
| | A | St. Dev | F |
| PM10 | 13113 | 4778 | 100% |
| S | 1684 | 933 | 67% |
| Cl | 209 | 376 | 38% |
| K | 340 | 291 | 65% |
| Ca | 151 | 120 | 93% |
| Ti | 31 | 19 | 98% |
| V | 16 | 13 | 95% |
| Cr | 10 | 5 | 58% |
| Mn | 5 | 4 | 75% |
| Fe | 164 | 101 | 98% |
| Ni | 7 | 5 | 87% |
| Cu | 5 | 3 | 64% |
| Zn | 16 | 15 | 87% |
| Br | 7 | 5 | 58% |
| Ba | 15 | 7 | 27% |
| Pb | 4 | 3 | 16% |
| OC | 3735 | 948 | 36% |
| EC | 443 | 284 | 95% |
| MSA | 54 | 28 | 93% |
| Cl ⁻ | 381 | 452 | 98% |
| NO ³⁻ | 882 | 584 | 98% |
| SO ₄ ²⁻ | 3216 | 2254 | 100% |
| Na ⁺ | 1003 | 566 | 100% |
| NH ₄ ⁺ | 1043 | 869 | 100% |
| K ⁺ | 151 | 150 | 27% |
| Mg ²⁺ | 139 | 79 | 100% |
| Ca ²⁺ | 222 | 114 | 100% |
| BC | 570 | 501 | 100% |

Table2[Click here to download Table: Table2.docx](#)

| ng m ⁻³ | July 18-25 | August 15-22 | September 12-19 |
|---|------------|--------------|-----------------|
| totSO₄²⁻ | 1750 | 4810 | 3100 |
| ssSO₄²⁻ | 360 | 140 | 190 |
| nssSO₄²⁻_{crustal} | 13 | 25 | 18 |
| nssSO₄²⁻_{biogenic} | 770 | 2070 | 430 |
| nssSO₄²⁻_{anthropogenic} | 650 | 2570 | 2460 |

Table3

[Click here to download Table: Table3.docx](#)

| Source | July 18-25 | | August 15-22 | | September 12-19 | |
|-----------------------------|-----------------------|--------|-----------------------|--------|-----------------------|--------|
| | (ng m ⁻³) | (%) | (ng m ⁻³) | (%) | (ng m ⁻³) | (%) |
| <i>Secondary Sulphate</i> | 730 ± 170 | 14 ± 3 | 5730 ± 720 | 41 ± 5 | 3730 ± 500 | 39 ± 5 |
| <i>Reacted dust</i> | 650 ± 40 | 12 ± 1 | 980 ± 80 | 7 ± 1 | 250 ± 40 | 3 ± 1 |
| <i>Biomass burning</i> | 540 ± 200 | 10 ± 4 | 3890 ± 600 | 28 ± 4 | 3170 ± 490 | 33 ± 5 |
| <i>Sea salt</i> | 2260 ± 330 | 43 ± 6 | 1740 ± 440 | 13 ± 3 | 1420 ± 380 | 15 ± 4 |
| <i>Heavy oil combustion</i> | 1110 ± 150 | 21 ± 3 | 1470 ± 410 | 11 ± 4 | 910 ± 410 | 10 ± 4 |

Figure1

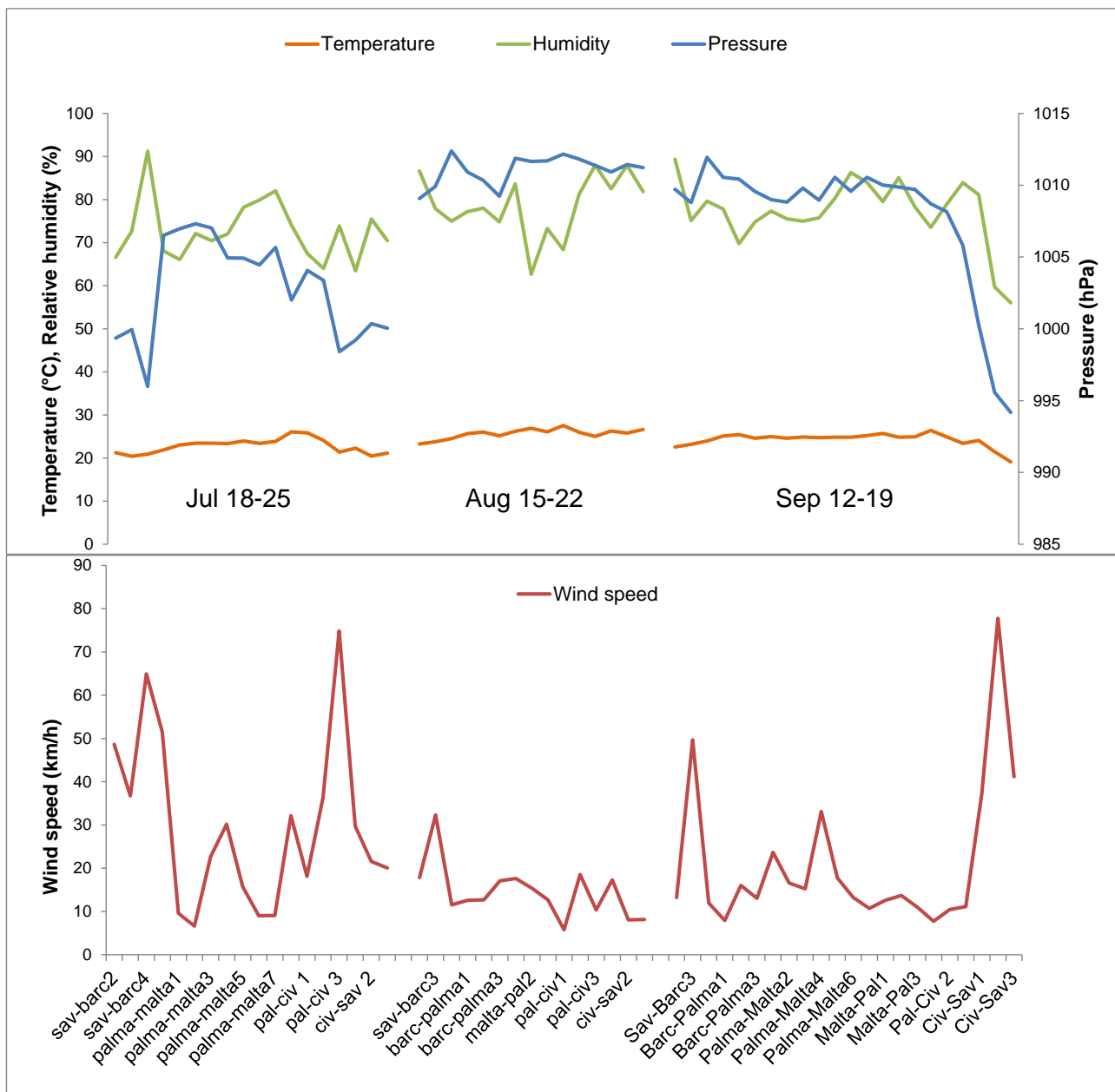


Figure2

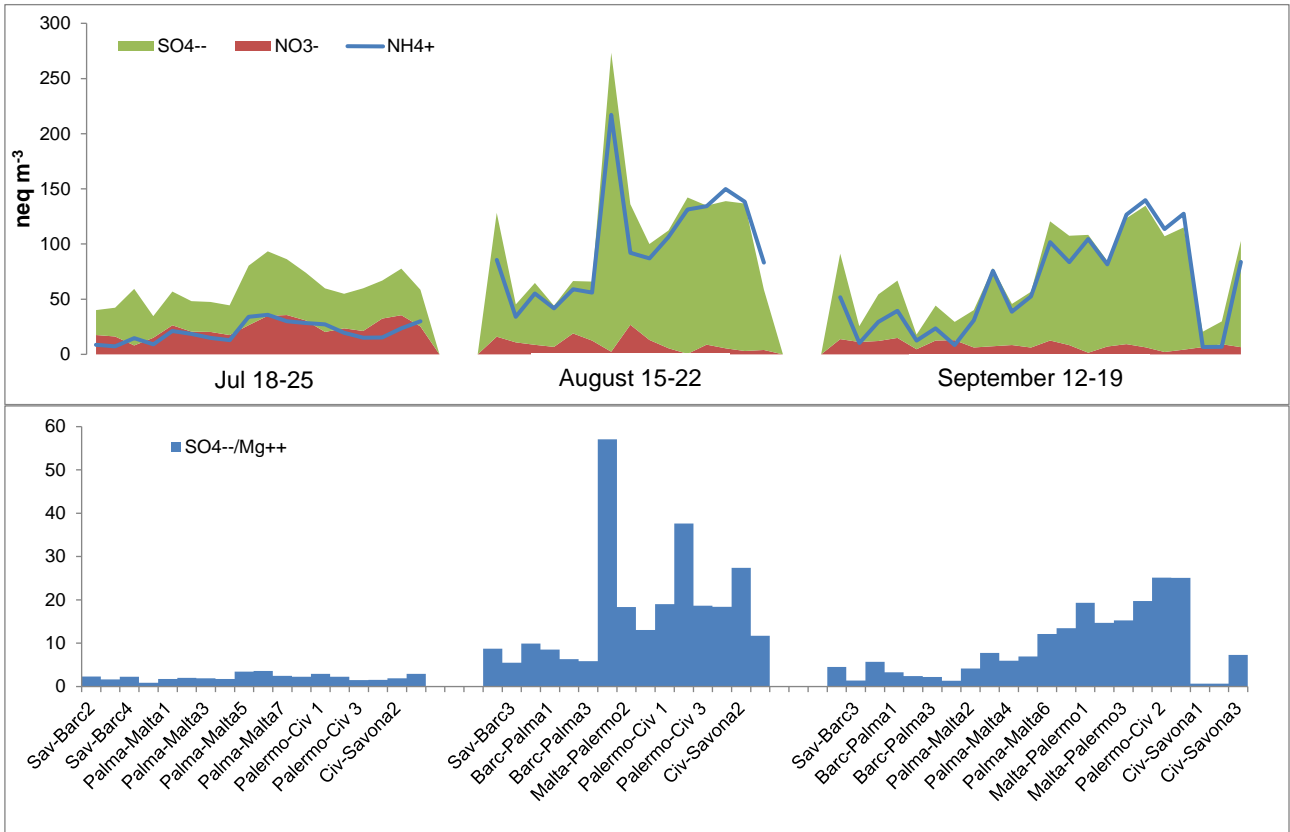


Figure3

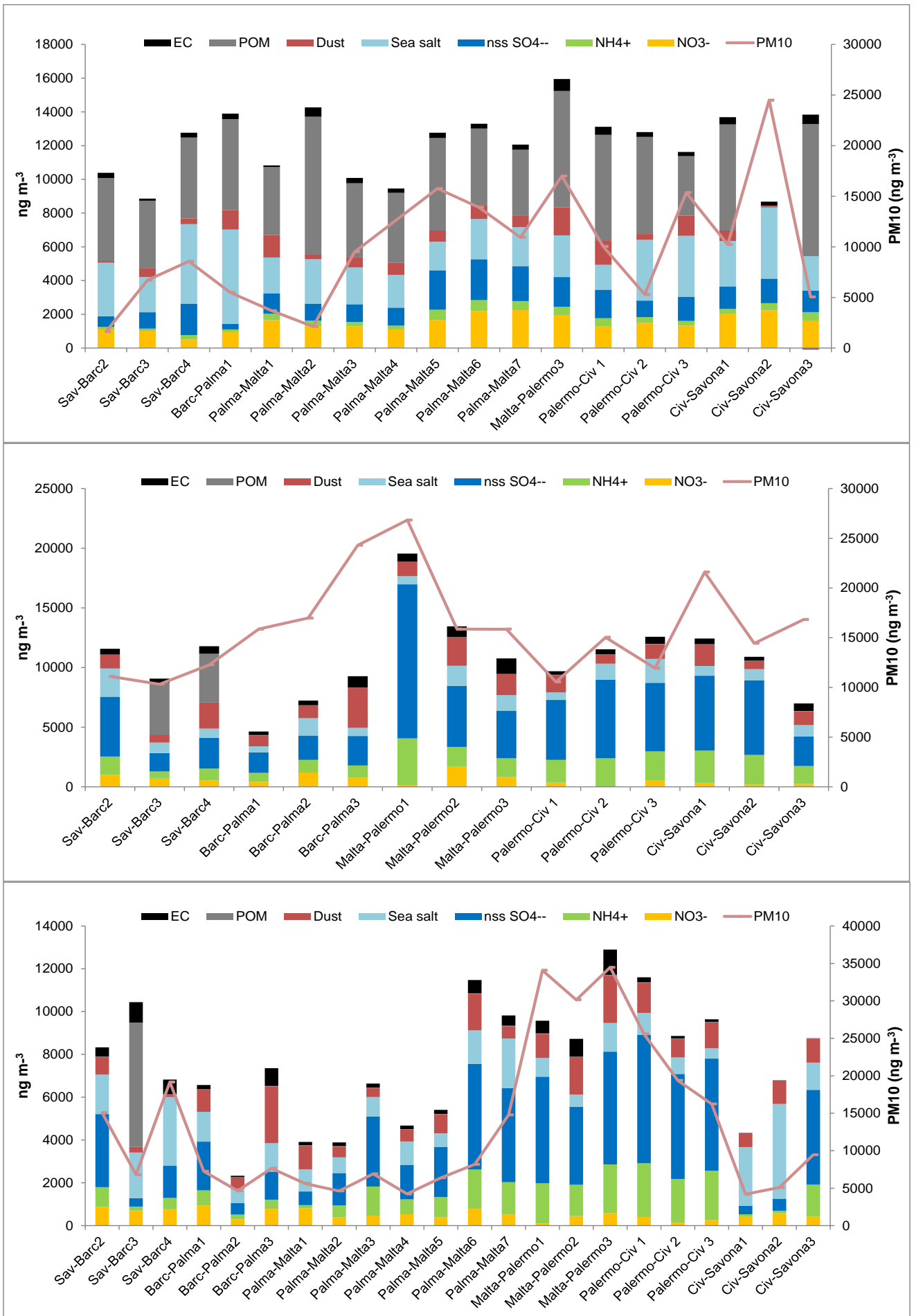
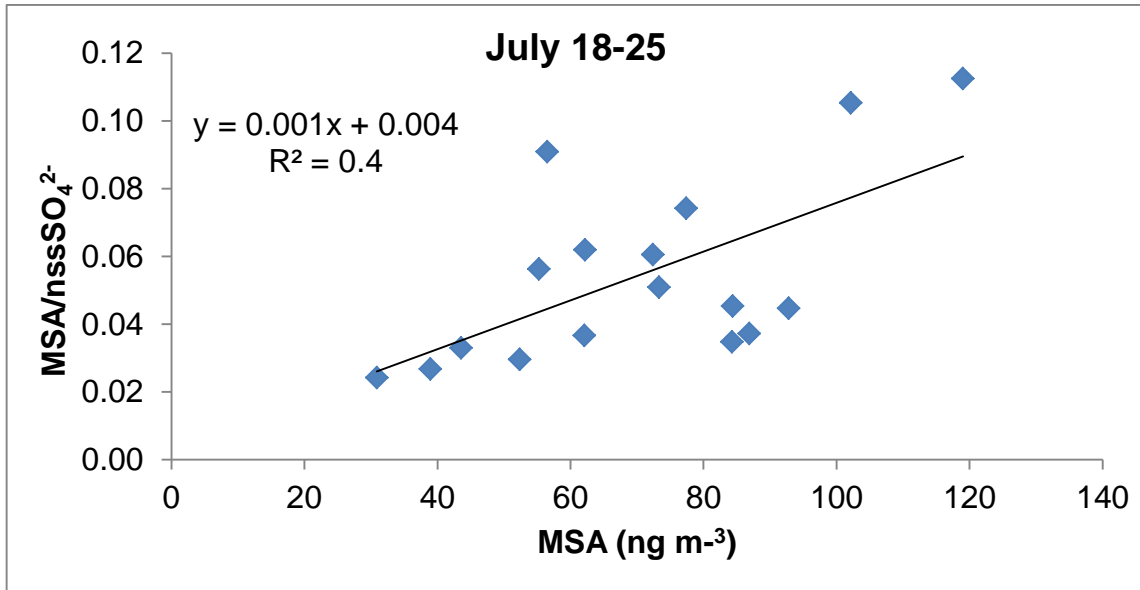
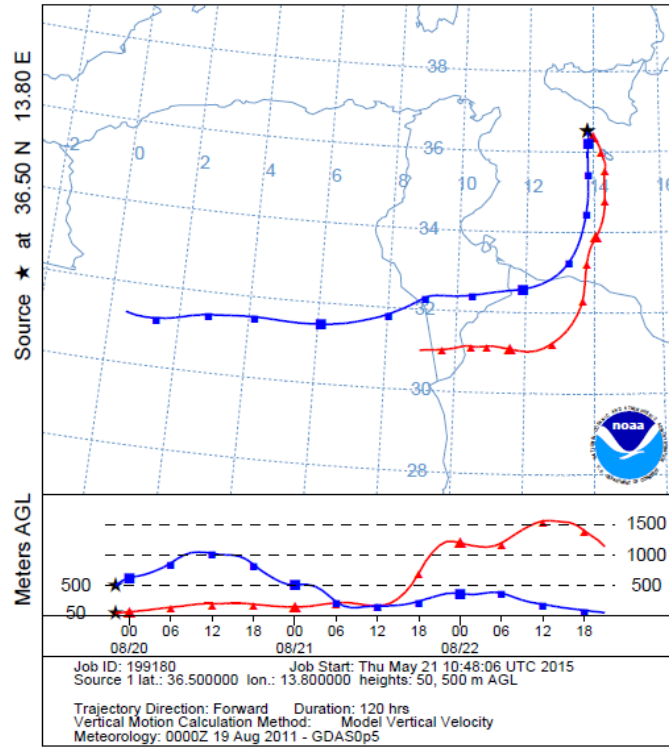


Figure4



NOAA HYSPLIT MODEL
 Forward trajectories starting at 2200 UTC 19 Aug 11
 GHDA Meteorological Data



NOAA HYSPLIT MODEL
 Backward trajectories ending at 0400 UTC 19 Jul 11
 GHDA Meteorological Data

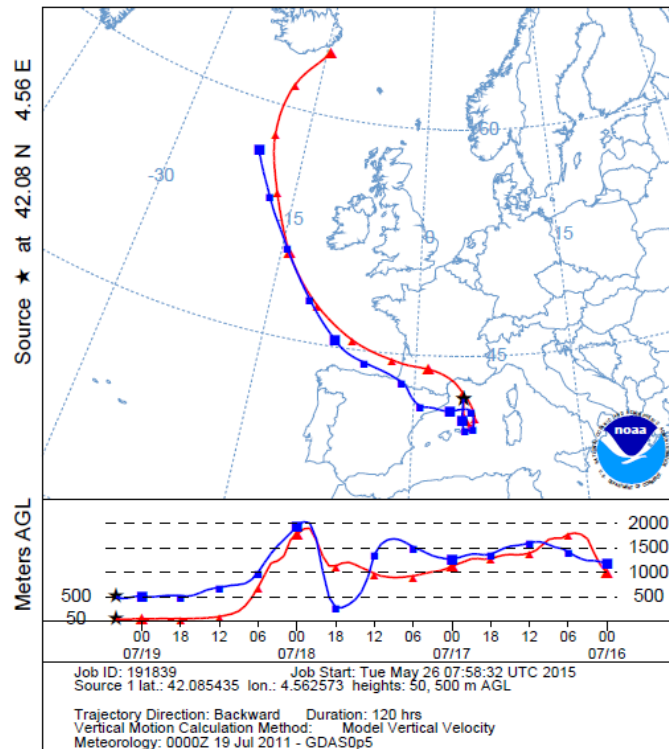


Figure6

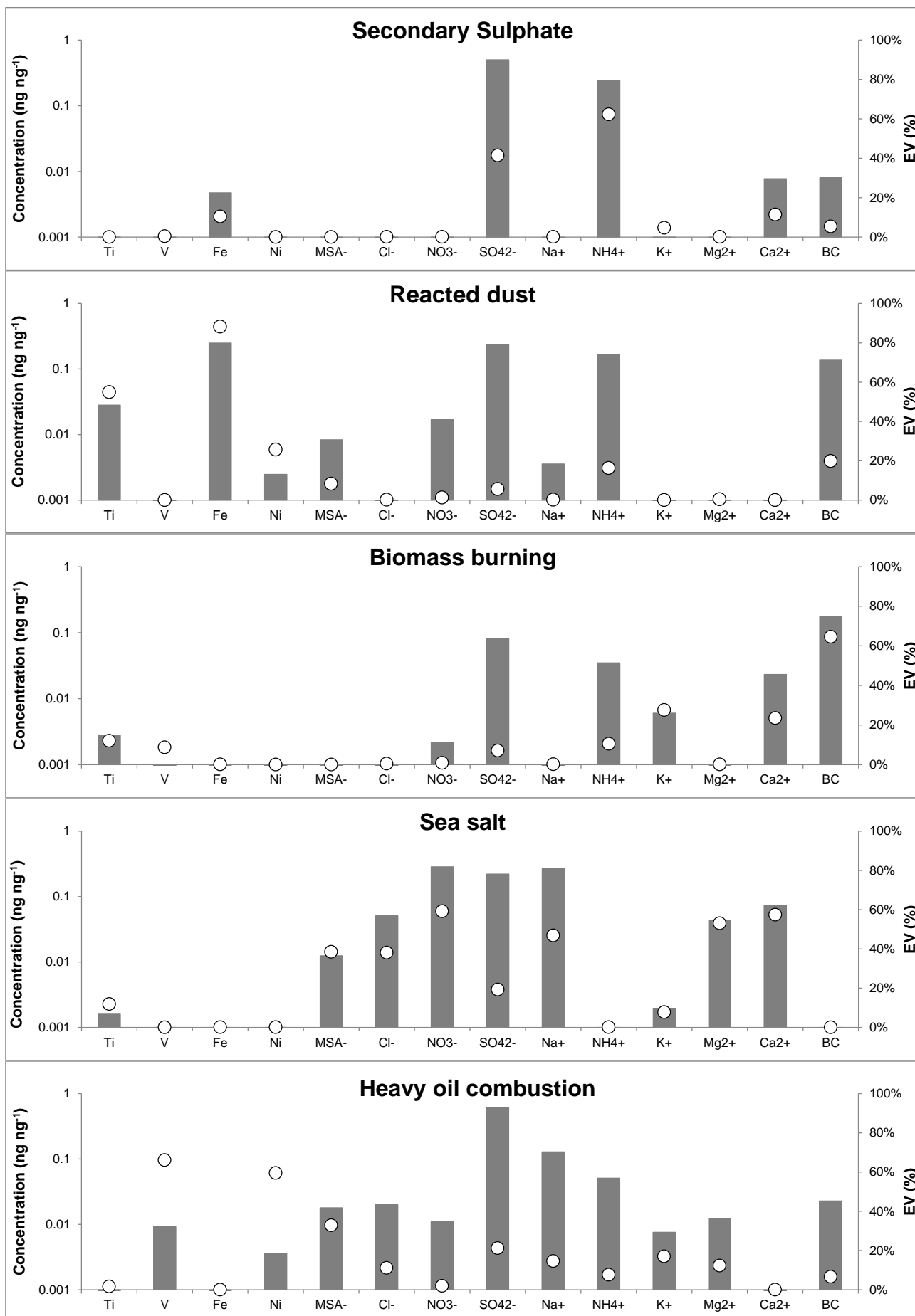


Figure7

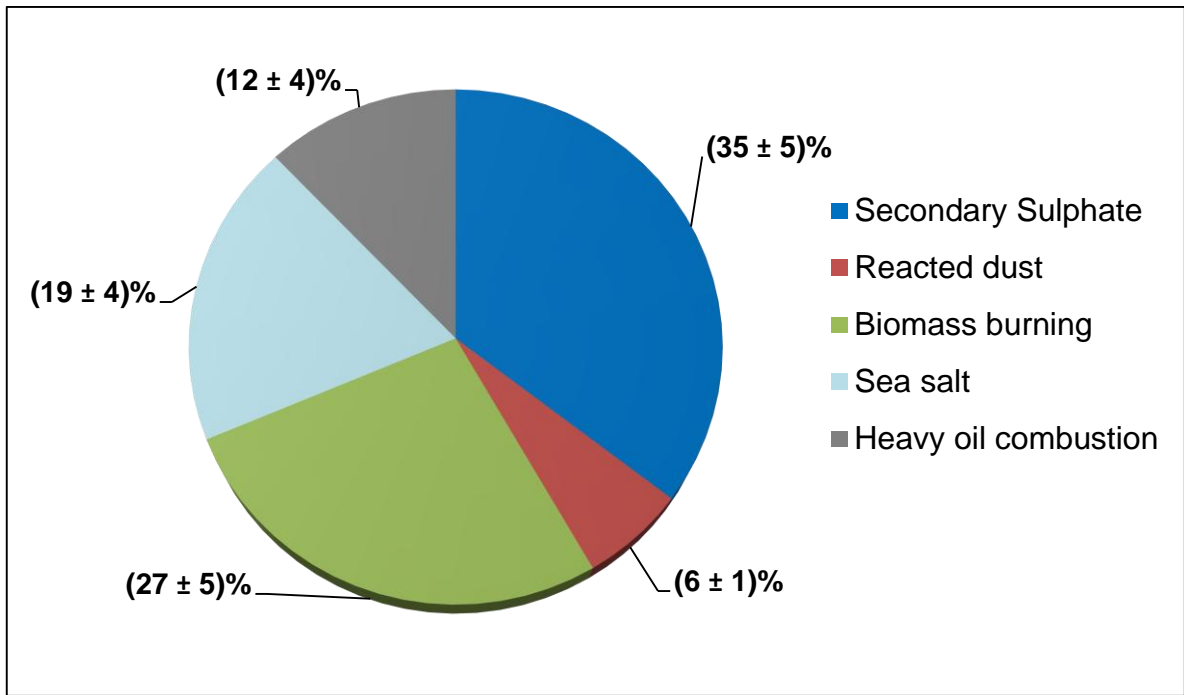
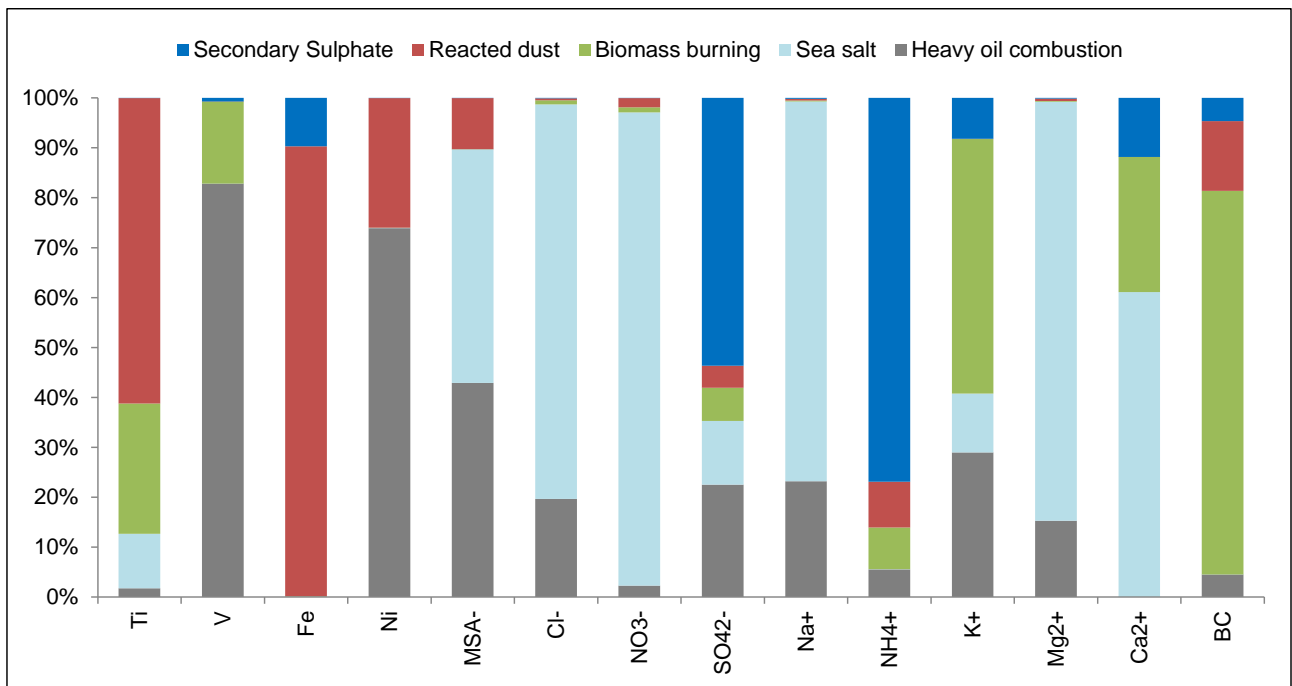


Figure8



Supplementary Material Fig E1

[Click here to download Supplementary Material: FigE1.docx](#)

Supplementary Material Fig E2

[Click here to download Supplementary Material: FigE2.docx](#)

Supplementary Material Fig E3

[Click here to download Supplementary Material: FigE3.docx](#)

Supplementary Material Fig E4

[Click here to download Supplementary Material: FigE4.docx](#)

Supplementary Material Fig E5

[Click here to download Supplementary Material: FigE5.docx](#)

Supplementary Material Fig E6

[Click here to download Supplementary Material: FigE6.docx](#)

Supplementary Material Fig E7

[Click here to download Supplementary Material: FigE7.docx](#)

Supplementary Material Fig E8

[Click here to download Supplementary Material: FigE8.docx](#)